A Collection of Edge-Based Elements

Leo C. Kempel and John L. Volakis
Radiation Laboratory
University of Michigan

January 5, 1992

Abstract

Edge-based elements have proved useful in solving electromagnetic problems since they are divergenceless. Previous authors have presented several two-dimensional and three-dimensional elements. Herein, we present four types of elements which are suitable for modeling several types of three-dimensional geometries. Distorted brick and triangular prism elements are given in cartesian coordinates as well as the specialized cylindrical shell and pie-shaped prism elements which are suitable for problems best described in polar cylindrical coordinates.

Contents

where $\bar{E}$ is the electric field and G is a Green's function. For the remainder of this report, we suppress the dependence of F on the unprimed coordinates since there will be no operations carried out in these coordinates. Furthermore, we express (1) in terms of its cartesian components

$$\bar{I} = \hat{x} I_x + \hat{y} I_y + \hat{z} I_z \tag{3}$$

where

$$I_\zeta = \hat{\zeta} \cdot \int_V \bar{F}(x', y', z')\, dx'\, dy'\, dz' \tag{4}$$

and $\zeta \in \{ x, y, z \}$.

To evaluate (4), we apply the change of variables theorem to map the original brick domain into the unit cube as shown in figure 1b.

$$I_\zeta = \hat{\zeta} \cdot \int_0^1 \int_0^1 \int_0^1 \bar{F}(x'(u,v,w), y'(u,v,w), z'(u,v,w)) |J(u,v,w)|\, du\, dv\, dw \tag{5}$$

which is accomplished by allowing

$$x'(u,v,w) = \sum_{i=1}^{8} N_i(u,v,w)\, x_i' \tag{6}$$

$$y'(u,v,w) = \sum_{i=1}^{8} N_i(u,v,w)\, y_i' \tag{7}$$

$$z'(u,v,w) = \sum_{i=1}^{8} N_i(u,v,w)\, z_i' \tag{8}$$

with (x_i', y_i', z_i') denoting the ith node coordinates as shown in figure 1a. The shape functions are given by

$$\begin{aligned}
N_1(u,v,w) &= (1-u)(1-v)(1-w) & N_5(u,v,w) &= (1-u)(1-v)w \\
N_2(u,v,w) &= u(1-v)(1-w) & N_6(u,v,w) &= u(1-v)w \\
N_3(u,v,w) &= uv(1-w) & N_7(u,v,w) &= uvw \\
N_4(u,v,w) &= (1-u)v(1-w) & N_8(u,v,w) &= (1-u)vw
\end{aligned} \tag{9}$$

and the Jacobian is of the form

$$\begin{aligned}
|J(u,v,w)| = {} & \frac{\partial x'}{\partial u}\frac{\partial y'}{\partial v}\frac{\partial z'}{\partial w} - \frac{\partial x'}{\partial u}\frac{\partial y'}{\partial w}\frac{\partial z'}{\partial v} - \frac{\partial y'}{\partial u}\frac{\partial x'}{\partial v}\frac{\partial z'}{\partial w} \\
& + \frac{\partial y'}{\partial u}\frac{\partial x'}{\partial w}\frac{\partial z'}{\partial v} + \frac{\partial z'}{\partial u}\frac{\partial x'}{\partial v}\frac{\partial y'}{\partial w} - \frac{\partial z'}{\partial u}\frac{\partial x'}{\partial w}\frac{\partial y'}{\partial v}
\end{aligned} \tag{10}$$

1 Introduction

Edge-based expansion functions have become popular in finite element and moment method techniques applied to the solution of electromagnetic scattering problems. This is due to the fact that the expansion functions are divergenceless within the element domain while any fictitious charges formed at the edges of the element will be canceled by another edge resulting in a volume which is divergenceless. In contrast, nodal expansion functions are not divergenceless and are thus less accurate.

Tanner and Peterson [1] presented triangular and tetrahedral divergenceless vector elements while Jin and Volakis [2] applied the corresponding rectangular brick elements to slot scattering problems. Kameari [3] presented distorted linear and quadratic brick elements in the context of transient quasi-magnetostatic problems.

In this report we derive edge-based expansion functions for a variety of three-dimensional elements. These expansion functions are characterized by unit value along one edge of the element while vanishing along all the remaining edges which are parallel to the unit edge. Distorted bricks, distorted triangular prisms, cylindrical shells and pie-shaped prisms will be presented. The first two of these are suited for completely general inhomogeneous domains whereas the last two are more appropriate for domains terminated at cylindrical boundaries.

2 Distorted Brick Element

The first element considered is the distorted brick which is shown in figure 1a. The strategy used herein is to first employ the change of variable theorem to convert the integration domain from the original distorted brick into a cube. Once this is accomplished, the vector-valued function may be expanded in terms of edge-based expansion functions as was done by Jin and Volakis[2]. Typically, one wishes to integrate some vector-valued function

$$\bar{I}(x,y,z) = \int_V \bar{F}(x',y',z',x,y,z)\,dx'\,dy'\,dz' \tag{1}$$

over the domain of the element where V is the volume of the brick and the vector valued integrand is typically of the form

$$\bar{F}(x',y',z') = \bar{E}(x',y',z')\,G(x',y',z',x,y,z) \tag{2}$$

where $\bar{E}$ is the electric field and G is a Green's function. For the remainder of this report, we suppress the dependence of F on the unprimed coordinates since there will be no operations carried out in these coordinates. Furthermore, we express (1) in terms of its cartesian components

$$\bar{I} = \hat{x} I_x + \hat{y} I_y + \hat{z} I_z \tag{3}$$

where

$$I_\zeta = \hat{\zeta} \cdot \int_V \bar{F}(x', y', z')\, dx'\, dy'\, dz' \tag{4}$$

and $\zeta \in \{ x, y, z \}$.

To evaluate (4), we apply the change of variables theorem to map the original brick domain into the unit cube as shown in figure 1b.

$$I_\zeta = \hat{\zeta} \cdot \int_0^1 \int_0^1 \int_0^1 \bar{F}(x'(u,v,w), y'(u,v,w), z'(u,v,w)) |J(u,v,w)|\, du\, dv\, dw \tag{5}$$

which is accomplished by allowing

$$x'(u,v,w) = \sum_{i=1}^{8} N_i(u,v,w)\, x_i' \tag{6}$$

$$y'(u,v,w) = \sum_{i=1}^{8} N_i(u,v,w)\, y_i' \tag{7}$$

$$z'(u,v,w) = \sum_{i=1}^{8} N_i(u,v,w)\, z_i' \tag{8}$$

with (x_i', y_i', z_i') denoting the ith node coordinates as shown in figure 1a. The shape functions are given by

$$\begin{aligned}
N_1(u,v,w) &= (1-u)(1-v)(1-w) & \qquad N_5(u,v,w) &= (1-u)(1-v)w \\
N_2(u,v,w) &= u(1-v)(1-w) & \qquad N_6(u,v,w) &= u(1-v)w \\
N_3(u,v,w) &= uv(1-w) & \qquad N_7(u,v,w) &= uvw \\
N_4(u,v,w) &= (1-u)v(1-w) & \qquad N_8(u,v,w) &= (1-u)vw
\end{aligned} \tag{9}$$

and the Jacobian is of the form

$$\begin{aligned}
|J(u,v,w)| = {} & \frac{\partial x'}{\partial u}\frac{\partial y'}{\partial v}\frac{\partial z'}{\partial w} - \frac{\partial x'}{\partial u}\frac{\partial y'}{\partial w}\frac{\partial z'}{\partial v} - \frac{\partial y'}{\partial u}\frac{\partial x'}{\partial v}\frac{\partial z'}{\partial w} \\
& + \frac{\partial y'}{\partial u}\frac{\partial x'}{\partial w}\frac{\partial z'}{\partial v} + \frac{\partial z'}{\partial u}\frac{\partial x'}{\partial v}\frac{\partial y'}{\partial w} - \frac{\partial z'}{\partial u}\frac{\partial x'}{\partial w}\frac{\partial y'}{\partial v}
\end{aligned} \tag{10}$$

The partial derivatives are computed from

$$\frac{\partial \zeta}{\partial \nu} = \sum_{i=1}^{8} \frac{\partial N_i}{\partial \nu}(u,v,w)\zeta_i \tag{11}$$

with $\zeta \in \{ x, y, z \}$ and $\nu \in \{ u, v, w \}$. From (9) the partial derivatives of the shape functions are found to be

$$\frac{\partial N_1(u,v,w)}{\partial u} = -(1-v)(1-w) \qquad \frac{\partial N_5(u,v,w)}{\partial u} = -(1-v)w$$

$$\frac{\partial N_2(u,v,w)}{\partial u} = (1-v)(1-w) \qquad \frac{\partial N_6(u,v,w)}{\partial u} = (1-v)w$$

$$\frac{\partial N_3(u,v,w)}{\partial u} = v(1-w) \qquad \frac{\partial N_7(u,v,w)}{\partial u} = vw$$

$$\frac{\partial N_4(u,v,w)}{\partial u} = -v(1-w) \qquad \frac{\partial N_8(u,v,w)}{\partial u} = -vw$$

$$\frac{\partial N_1(u,v,w)}{\partial v} = -(1-u)(1-w) \qquad \frac{\partial N_5(u,v,w)}{\partial v} = -(1-u)w$$

$$\frac{\partial N_2(u,v,w)}{\partial v} = -u(1-w) \qquad \frac{\partial N_6(u,v,w)}{\partial v} = -uw$$

$$\frac{\partial N_3(u,v,w)}{\partial v} = u(1-w) \qquad \frac{\partial N_7(u,v,w)}{\partial v} = uw$$

$$\frac{\partial N_4(u,v,w)}{\partial v} = (1-u)(1-w) \qquad \frac{\partial N_8(u,v,w)}{\partial v} = (1-u)w$$

$$\frac{\partial N_1(u,v,w)}{\partial w} = -(1-u)(1-v) \qquad \frac{\partial N_5(u,v,w)}{\partial w} = (1-u)(1-v)$$

$$\frac{\partial N_2(u,v,w)}{\partial w} = -u(1-v) \qquad \frac{\partial N_6(u,v,w)}{\partial w} = u(1-v)$$

$$\frac{\partial N_3(u,v,w)}{\partial w} = -uv \qquad \frac{\partial N_7(u,v,w)}{\partial w} = uv$$

$$\frac{\partial N_4(u,v,w)}{\partial w} = -(1-u)v \qquad \frac{\partial N_8(u,v,w)}{\partial w} = (1-u)v$$

Now that we have transformed the integration domain from the original distorted brick into the unit cube, we may expand the vector-valued integral in terms of an edge-based expansion of the form

$$\bar{F}(x'(u,v,w), y'(u,v,w), z'(u,v,w)) = \sum_{j=1}^{12} \bar{N}_j^e(u,v,w)\psi_j \tag{12}$$

where

$$\begin{aligned}
\bar{N}_1^e(u,v,w) &= (1-v)(1-w)\hat{t}_{12} & \bar{N}_7^e(u,v,w) &= u(1-w)\hat{t}_{58} \\
\bar{N}_2^e(u,v,w) &= v(1-w)\hat{t}_{43} & \bar{N}_8^e(u,v,w) &= uw\hat{t}_{67} \\
\bar{N}_3^e(u,v,w) &= (1-v)w\hat{t}_{56} & \bar{N}_9^e(u,v,w) &= (1-u)(1-v)\hat{t}_{15} \\
\bar{N}_4^e(u,v,w) &= vw\hat{t}_{87} & \bar{N}_{10}^e(u,v,w) &= u(1-v)\hat{t}_{26} \\
\bar{N}_5^e(u,v,w) &= (1-u)(1-w)\hat{t}_{14} & \bar{N}_{11}^e(u,v,w) &= (1-u)v\hat{t}_{48} \\
\bar{N}_6^e(u,v,w) &= (1-u)w\hat{t}_{23} & \bar{N}_{12}^e(u,v,w) &= uv\hat{t}_{37}
\end{aligned} \tag{13}$$

in which ψ_j are the unknown expansion coefficients and $\hat{t}_{ij}$ denote the element's unit edge vectors given by

$$\hat{t}_{ij} = \frac{\bar{r}_j - \bar{r}_i}{|\bar{r}_j - \bar{r}_i|} \tag{14}$$

with $\bar{r}_j$ being the position vectors in the original domain.

We may now express the cartesian components of (3) as

$$I_\zeta = \hat{\zeta} \cdot \sum_{j=1}^{12} \psi_j \int_0^1 \int_0^1 \int_0^1 \bar{N}_j^e(u,v,w)|J(u,v,w)|\, du\, dv\, dw \tag{15}$$

recognizing that ψ_j represents the average component of the vector-valued function associated with the jth edge.

It should be noted that the brick cannot be too distorted. This is due to the change of variables theorem. In order to assure a one-to-one mapping for (x,y,z) to (u,v,w), the sign of the Jacobian may not change. This condition will preclude elements that are twisted or extremely narrow and diamond shaped. The typical element should therefore not deviate much from the rectangular brick.

3 Distorted Triangular Prism

A triangular prism element such as the one shown in figure 2a may be developed in exactly the same manner as the brick. In this case, we employ a mapping from the original volume V to the volume shown in figure 2b followed by an edge-based expansion of the vector-valued integrand. The cartesian component integral may be expressed as

$$I_\zeta = \hat{\zeta} \cdot \int_0^1 \int_0^1 \int_0^{1-u} \bar{F}(x'(u,v,w), y'(u,v,w), z'(u,v,w)) |J(u,v,w)| \, dv \, du \, dw \tag{16}$$

where the coordinate mapping is given by

$$x'(u,v,w) = \sum_{i=1}^{6} N_i(u,v,w) \, x'_i \tag{17}$$

$$y'(u,v,w) = \sum_{i=1}^{6} N_i(u,v,w) \, y'_i \tag{18}$$

$$z'(u,v,w) = \sum_{i=1}^{6} N_i(u,v,w) \, z'_i \tag{19}$$

with the node coordinates (x'_i, y'_i, z'_i) shown in figure 2a and the shape functions are given by

$$\begin{aligned} N_1(u,v,w) &= (1-u-v)(1-w) & \qquad N_4(u,v,w) &= (1-u-v)w \\ N_2(u,v,w) &= u(1-w) & \qquad N_5(u,v,w) &= uw \\ N_3(u,v,w) &= v(1-w) & \qquad N_6(u,v,w) &= vw \end{aligned} \tag{20}$$

The Jacobian is again given by (10) with

$$\frac{\partial \zeta}{\partial \nu} = \sum_{i=1}^{6} \frac{\partial N_i}{\partial \nu}(u,v,w) \zeta_i \tag{21}$$

and the non-zero shape partial derivatives of N_i are

$$\begin{aligned}
\frac{\partial N_1}{\partial u} &= -(1-w) = \frac{\partial N_1}{\partial v} & \frac{\partial N_1}{\partial w} &= -(1-u-v) = -\frac{\partial N_4}{\partial w} \\
\frac{\partial N_2}{\partial u} &= (1-w) = \frac{\partial N_3}{\partial v} & \frac{\partial N_2}{\partial w} &= -u = -\frac{\partial N_5}{\partial w} \\
\frac{\partial N_4}{\partial u} &= -w = \frac{\partial N_4}{\partial v} & \frac{\partial N_3}{\partial w} &= -v = -\frac{\partial N_6}{\partial w} \\
\frac{\partial N_5}{\partial u} &= w = \frac{\partial N_6}{\partial v}
\end{aligned} \tag{22}$$

The vector valued function in (16) is expanded in terms of edge-based functions

$$\bar{F}(x'(u,v,w), y'(u,v,w), z'(u,v,w)) = \sum_{j=1}^{9} \bar{N}_j^e(u,v,w)\,\psi_j \tag{23}$$

where the vector expansion functions are

$$\begin{aligned}
\bar{N}_1^e(u,v,w) &= [(\xi_1+\xi_2)\hat{t}_{12} + \xi_2\hat{t}_{13}](1-w) \\
\bar{N}_2^e(u,v,w) &= -\sqrt{2}[\xi_3\hat{t}_{12} - \xi_2\hat{t}_{13}](1-w) \\
\bar{N}_3^e(u,v,w) &= -[\xi_3\hat{t}_{12} + (\xi_1+\xi_3)\hat{t}_{13}](1-w) \\
\bar{N}_4^e(u,v,w) &= [(\xi_1+\xi_2)\hat{t}_{45} + \xi_2\hat{t}_{46}]w \\
\bar{N}_5^e(u,v,w) &= -\sqrt{2}[\xi_3\hat{t}_{45} + \xi_2\hat{t}_{46}]w \\
\bar{N}_6^e(u,v,w) &= -[\xi_3\hat{t}_{45} + (\xi_1+\xi_3)\hat{t}_{46}]w \\
\bar{N}_7^e(u,v,w) &= u(1-v)\hat{t}_{25} \\
\bar{N}_8^e(u,v,w) &= (1-u)(1-v)\hat{t}_{14} \\
\bar{N}_9^e(u,v,w) &= (1-u)v\hat{t}_{36}
\end{aligned} \tag{24}$$

where the area coordinates in (24) are given for the new integration domain

$$\begin{aligned}
&\xi_n = 2\sqrt{s_n(s_n-a_n)(s_n-b_n)(s_n-c_n)} \\
&s_n = \frac{1}{2}(a_n+b_n+c_n) \\
&n \in \{1,2,3\}
\end{aligned} \tag{25}$$

and

$$\begin{array}{lllllll} a_1 &=& \sqrt{(u-1)^2+v^2} & a_2 &=& \sqrt{u^2+(v-1)^2} & a_3 &=& \sqrt{u^2+v^2} \\ b_1 &=& \sqrt{u^2+(v-1)^2} & b_2 &=& \sqrt{u^2+v^2} & b_3 &=& \sqrt{(u-1)^2+v^2} \\ c_1 &=& \sqrt{2} & c_2 &=& 1 & c_3 &=& 1 \end{array} \tag{26}$$

We are now able to express (16) as

$$I_\zeta = \sum_{j=1}^{9} \psi_j \int_0^1 \int_0^1 \int_0^{1-u} \bar{N}_j^e(u,v,w) |J(u,v,w)| \, dv \, du \, dw \tag{27}$$

realizing that the same limited distortion constraint exists for the triangular prism as was the case for the brick.

4 Cylindrical Shell Edge-Based Elements

Although the brick and triangular prism elements given previously are quite general, we find it advantageous to develop an element which is designed for cylindrical problems. The resulting formulation will be quite compact compared to the brick for example since a specific geometry is assumed. This element is the polar cylindrical coordinate equivalent of the brick introduced by Jin and Volakis [2] and is shown in figure 3.

For cylindrical problems, we wish to evaluate the integral

$$\bar{I} = \int_{z_1}^{z_5} \int_{\phi_1}^{\phi_2} \int_{\rho_1}^{\rho_4} \bar{F}(\rho', \phi', z') \rho' \, d\rho' \, d\phi' \, dz' \tag{28}$$

where the vector-valued function $\bar{F}(\rho', \phi', z')$ is analogous to (2). We do not employ any change of variable for this element so we may directly express the vector-valued function in terms of an edge-based expansion

$$\bar{F}(\rho', \phi', z') = \sum_{j=1}^{12} \bar{N}_j^e(\rho', \phi', z') \, \psi_j \tag{29}$$

The shape functions are given by

$$\bar{N}_1^e(\rho', \phi', z') = \left[\frac{\rho_4^2 - \rho'^2}{\rho_4^2 - \rho_1^2}\right] \left[\frac{z' - z_5}{z_1 - z_5}\right] \hat{\phi}$$

$$
\begin{aligned}
\bar{N}_2^e(\rho',\phi',z') &= \left[1-\frac{|\phi_2-\phi'|}{|\phi_2-\phi_1|}\right]\left[\frac{z'-z_5}{z_1-z_5}\right]\hat{\rho} \\
\bar{N}_3^e(\rho',\phi',z') &= \left[\frac{\rho'^2-\rho_1^2}{\rho_4^2-\rho_1^2}\right]\left[\frac{z'-z_5}{z_1-z_5}\right]\hat{\phi} \\
\bar{N}_4^e(\rho',\phi',z') &= \left[1-\frac{|\phi'-\phi_1|}{|\phi_2-\phi_1|}\right]\left[\frac{z'-z_5}{z_1-z_5}\right]\hat{\rho} \\
\bar{N}_5^e(\rho',\phi',z') &= \left[\frac{\rho_4^2-\rho'^2}{\rho_4^2-\rho_1^2}\right]\left[\frac{z'-z_1}{z_1-z_5}\right]\hat{\phi} \\
\bar{N}_6^e(\rho',\phi',z') &= \left[1-\frac{|\phi_2-\phi'|}{|\phi_2-\phi_1|}\right]\left[\frac{z'-z_1}{z_5-z_1}\right]\hat{\rho} \\
\bar{N}_7^e(\rho',\phi',z') &= \left[\frac{\rho'^2-\rho_1^2}{\rho_4^2-\rho_1^2}\right]\left[\frac{z'-z_1}{z_5-z_1}\right]\hat{\phi} \\
\bar{N}_8^e(\rho',\phi',z') &= \left[1-\frac{|\phi'-\phi_1|}{|\phi_2-\phi_1|}\right]\left[\frac{z'-z_1}{z_5-z_1}\right]\hat{\rho} \\
\bar{N}_9^e(\rho',\phi',z') &= \left[\frac{\rho_4-\rho'}{\rho_4-\rho_1}\right]\left[\frac{|\phi_2-\phi'|}{|\phi_2-\phi_1|}\right]\hat{z} \\
\bar{N}_{10}^e(\rho',\phi',z') &= \left[\frac{\rho_4-\rho'}{\rho_4-\rho_1}\right]\left[\frac{|\phi'-\phi_1|}{|\phi_2-\phi_1|}\right]\hat{z} \\
\bar{N}_{11}^e(\rho',\phi',z') &= \left[\frac{\rho'-\rho_1}{\rho_4-\rho_1}\right]\left[\frac{|\phi'-\phi_1|}{|\phi_2-\phi_1|}\right]\hat{z} \\
\bar{N}_{12}^e(\rho',\phi',z') &= \left[\frac{\rho'-\rho_1}{\rho_4-\rho_1}\right]\left[\frac{|\phi_2-\phi'|}{|\phi_2-\phi_1|}\right]\hat{z}
\end{aligned} \tag{30}
$$

where (ρ_i, ϕ_i, z_i) denote the node coordinates as shown in figure 3 and (28) is given by

$$
\bar{I} = \sum_{j=1}^{12} \psi_j \int_{z_1}^{z_5}\int_{\phi_1}^{\phi_2}\int_{\rho_1}^{\rho_4} \bar{N}_j^e(\rho',\phi',z')\,\rho'\,d\rho'\,d\phi'\,dz' \tag{31}
$$

5 Pie-Shaped Prism

The final element considered is the complement to the cylindrical shell element, the pie-shaped element which is shown in figure 4. The development of this element closely parallels the previous element.

The vector-valued integral is given by

$$\bar{I} = \int_{z_1}^{z_5} \int_{\phi_2}^{\phi_3} \int_{\rho_1}^{\rho_2} \bar{F}(\rho', \phi', z')\, \rho'\, d\rho'\, d\phi'\, dz' \tag{32}$$

The vector-valued function is expanded in terms of edge vectors

$$\bar{F}(\rho', \phi', z') = \sum_{j=1}^{9} \bar{N}_j^e(\rho', \phi', z')\, \psi_j \tag{33}$$

and the edge-based expansion functions are

$$\begin{aligned}
\bar{N}_1^e(\rho', \phi', z') &= \left[1 - \frac{|\phi' - \phi_2|}{|\phi_3 - \phi_2|}\right] \left[\frac{z_4 - z'}{z_4 - z_1}\right] \hat{\rho} \\
\bar{N}_2^e(\rho', \phi', z') &= \left[\frac{\rho' - \rho_1}{\rho_4 - \rho_1}\right] \left[\frac{z_4 - z'}{z_4 - z_1}\right] \hat{\phi} \\
\bar{N}_3^e(\rho', \phi', z') &= \left[1 - \frac{|\phi_3 - \phi'|}{|\phi_3 - \phi_2|}\right] \left[\frac{z_4 - z'}{z_4 - z_1}\right] \hat{\rho} \\
\bar{N}_4^e(\rho', \phi', z') &= \left[1 - \frac{|\phi' - \phi_2|}{|\phi_3 - \phi_2|}\right] \left[\frac{z' - z_1}{z_4 - z_1}\right] \hat{\rho} \\
\bar{N}_5^e(\rho', \phi', z') &= \left[\frac{\rho' - \rho_1}{\rho_2 - \rho_1}\right] \left[\frac{z' - z_1}{z_4 - z_1}\right] \hat{\phi} \\
\bar{N}_6^e(\rho', \phi', z') &= \left[1 - \frac{|\phi_3 - \phi'|}{|\phi_3 - \phi_2|}\right] \left[\frac{z' - z_1}{z_4 - z_1}\right] \hat{\rho} \\
\bar{N}_7^e(\rho', \phi', z') &= \left[\frac{\rho' - \rho_1}{\rho_2 - \rho_1}\right] \left[\frac{|\phi_3 - \phi'|}{|\phi_3 - \phi_2|}\right] \hat{z} \\
\bar{N}_8^e(\rho', \phi', z') &= \left[\frac{\rho' - \rho_1}{\rho_2 - \rho_1}\right] \left[\frac{|\phi' - \phi_2|}{|\phi_3 - \phi_2|}\right] \hat{z} \\
\bar{N}_9^e(\rho', \phi', z') &= \left[\frac{\rho_2 - \rho'}{\rho_2 - \rho_1}\right] \hat{z}
\end{aligned} \tag{34}$$

where (ρ_i, ϕ_i, z_i) are the nodal coordinates shown in figure 4. With this expansion, (32) may be written

$$\bar{I} = \sum_{j=1}^{9} \psi_j \int_{z_1}^{z_5} \int_{\phi_2}^{\phi_3} \int_{\rho_1}^{\rho_2} \bar{N}_j^e(\rho', \phi', z')\, \rho'\, d\rho'\, d\phi'\, dz' \tag{35}$$

6 Conclusions

Four different linear volume elements were presented: distorted brick, distorted triangular prism, cylindrical shell, and pie-shaped prism. All of these elements are used to evaluate a vector-valued integral over the volume of the element by employing edge-based vector expansion functions. These functions were explicitly given for all elements. In addition, the shape functions and Jacobian associated with the mapping of the arbitrary brick or triangular prism to a known prism are presented. Since these elements are divergenceless, we expect them to useful for simulating various geometries via the finite element method or the Method of Moments.

References

[1] David R. Tanner and Andrew F. Peterson, "Vector Expansion Functions for the Numerical Solution of Maxwell's Equations," *Microwave and Optical Tech. Letters*, Sept. 1989.

[2] Jian-Ming Jin and John L. Volakis, "Electromagnetic Scattering by and Transmission Through a Three-Dimensional Slot in a Thick Conducting Plane," *IEEE Trans. Antennas Propagat.*, Vol. 39, No. 4, Apr. 1991.

[3] Akihisa Kameari, "Calculation of Transient 3D Eddy Current using Edge-Elements," *IEEE Trans. Magnetics*, Vol. 26, No. 2, Mar. 1990.

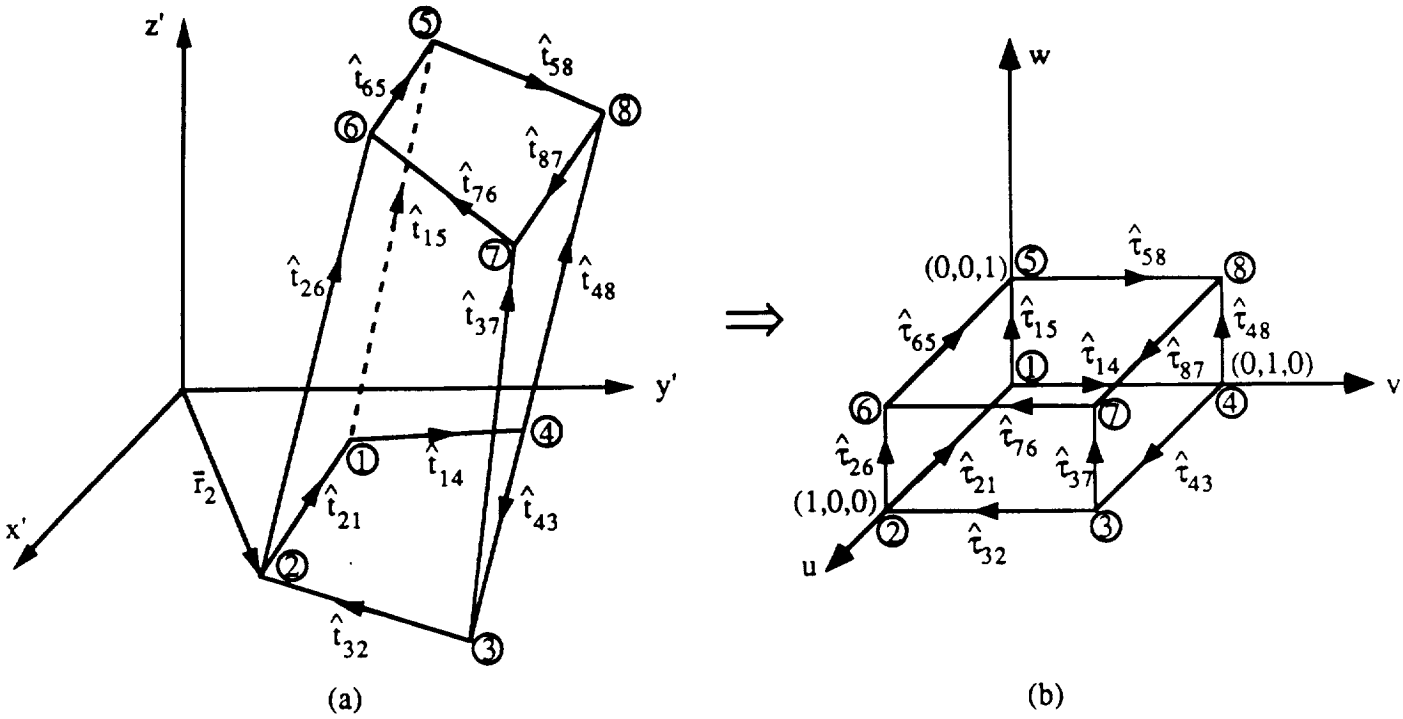

Figure 1

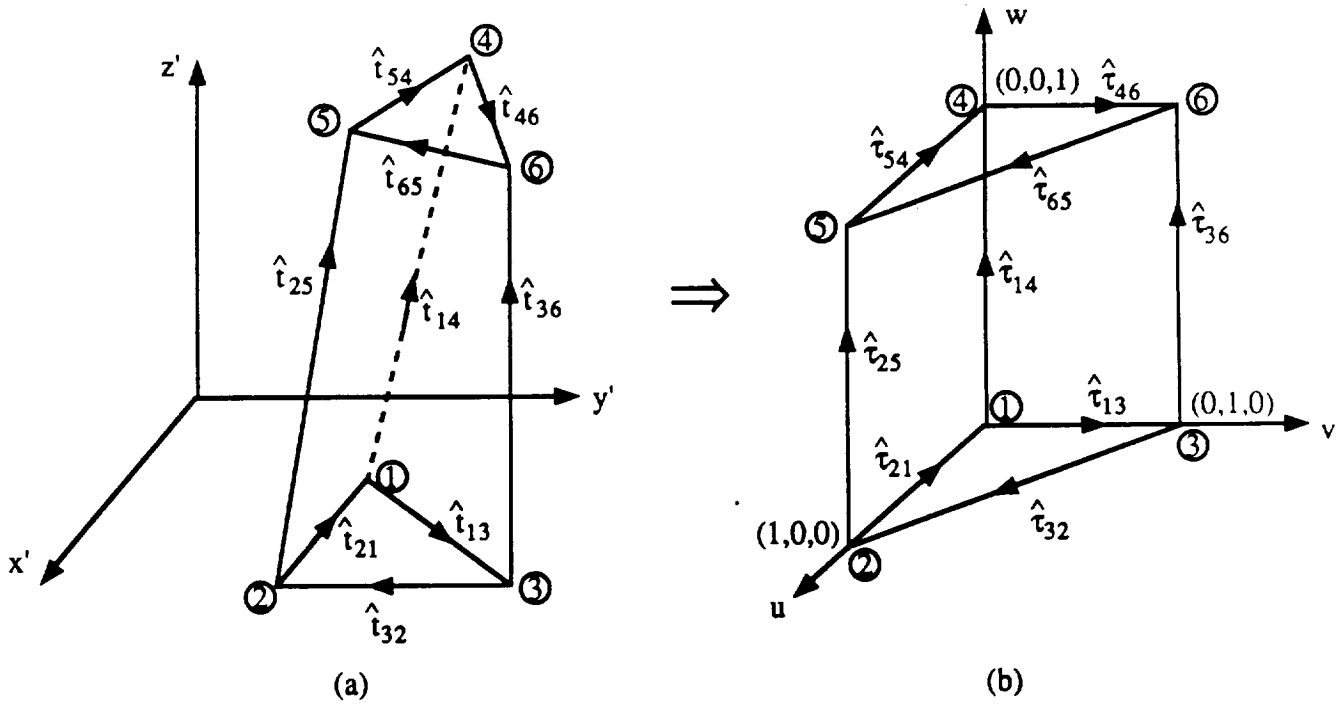

Figure 2

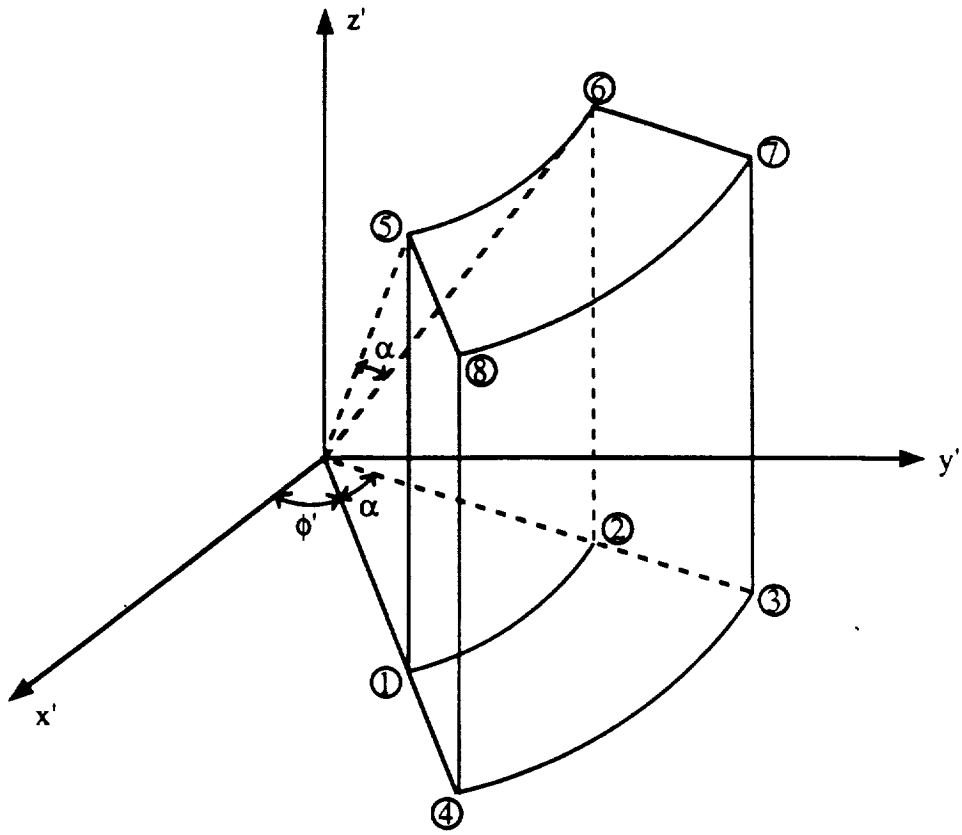

Figure 3

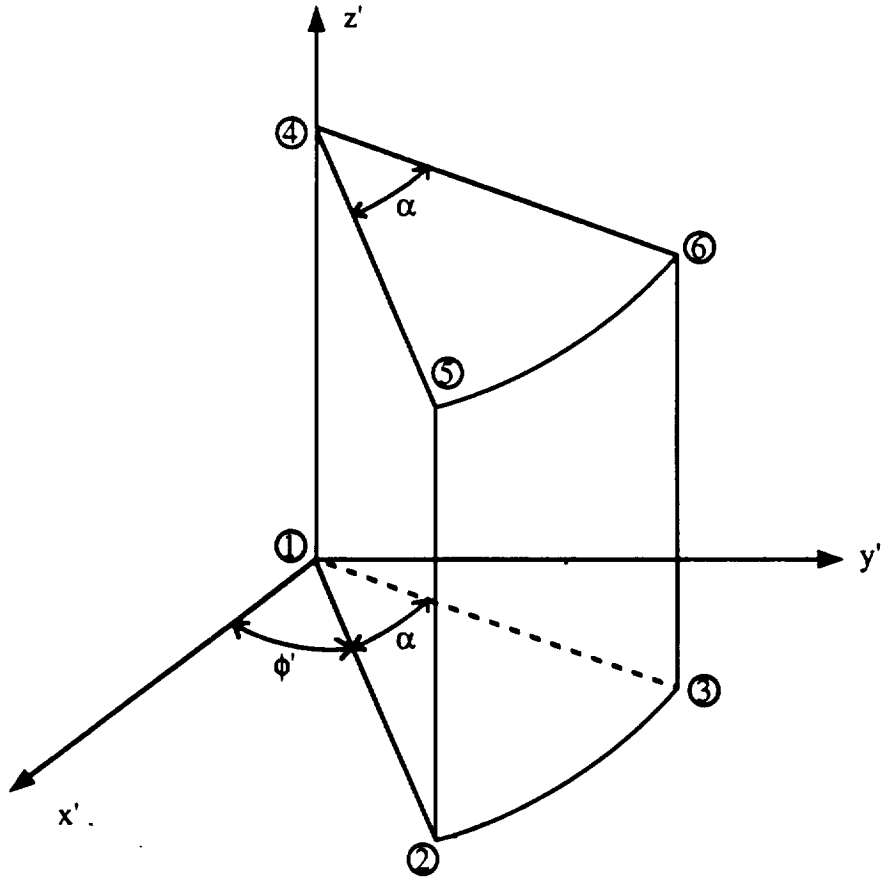

Figure 4